# Multi-maneuvers algorithms for multi-risk collision avoidance via nonconvex quadratic optimization

Matthieu Masson, Denis Arzelier, Mioara Joldes, Bruno Revelin, Jérôme Thomassin

# Multi-maneuvers algorithms for multi-risk collision avoidance via nonconvex quadratic optimization ⋆

**Matthieu Masson** * **Denis Arzelier** * **Mioara Joldes** * **Bruno Revelin** ** **Jérôme Thomassin** ***

* *LAAS-CNRS, Université de Toulouse 31400 Toulouse, France,*
matthieu.masson,arzelier,joldes@laas.fr.
** *Thales Services Numeriques, 290, All. du Lac 31670 Labège, France,*
bruno.revelin@thalesgroup.com.
*** *CNES, 18 Av. Edouard Belin, 31400 Toulouse, France,*
Jerome.Thomassin@cnes.fr.

Abstract: In this article, the problem of modeling and computing the optimal collision avoidance maneuvers for multiple short-term encounters is presented. Several metrics defining the overall collision risk are analyzed. These include imposing lower bounds on the miss-distance or the Mahalanobis distance at each corresponding time of closest approach (TCA) or upper-bounds on the orbital collision probability. The avoidance maneuvers are modeled as impulsive ones in a single direction of the local frame and for *a priori* fixed dates for operational motivations. Station-keeping constraints are also imposed via linear inequalities on the relative states at each TCA. The specific nature of the imposed constraints is dictated by a practical framework provided by the French Space Agency (CNES). This results in formulating the maneuver design problem as an optimization problem with linear objective and nonconvex quadratic constraints. Different algorithms are presented to solve this problem. Finally, the relative efficiency of the proposed approaches is evaluated and analyzed on two realistic conjunctions built from data extracted from the CNES database and on academic examples of higher complexity.

*Keywords:* Collision Avoidance Maneuver, Multiple Short-term Encounters, Impulsive Maneuvers, Quadratically Constrained Nonconvex Optimization

## 1. INTRODUCTION

Nowadays the risk of orbital collision for controlled satellites, especially in low orbits, needs to be assessed and mitigated by space agencies and owners/operators (O/O) of the field. When the predicted risk is too high according to mission requirements, a collision avoidance strategy usually consists in one or several evasive maneuvers. These are planned by taking into account both fuel consumption minimization (for preserving the lifetime of the satellite) and other operational constraints, like station-keeping by the time the threat is gone. More demanding operational constraints like disjunctive thrusts, minimum elapsed time between two thrusts, saturation constraints, etc., are often necessary when low-thrust (or electric) propulsion is used.

In this study, the collision avoidance problem between one active low-thrust satellite involved in short-term encounters with several uncontrolled objects, is considered. The active satellite, also called primary $p$, is initially set on a reference orbit. The other involved objects, called secondaries $s_j$, with $j = 1,\ldots,N$, are assumed to be uncontrolled space debris. The use of low-thrust propulsion is modeled, like in the work of Hennes et al. (2016), by a sequence of impulsive thrusts on specifically imposed thrust ranges over which the thrust magnitude is spread. Furthermore, due to the lack of precision in measurements, the quantification of the collision risk is also a difficult task and different risk assessment indicators include, for each pair $(p,s_j)$: (1) the miss-distance at the Time of Closest Approach (TCA); (2) the Mahalanobis miss-distance at TCA; (3) the short-term or (4) maximum collision probability (see for instance Fernández-Mellado and Vasile (2021) and Sec. 2 for details).

Hence, in this context, the collision avoidance problem is formulated as a constrained optimization problem: it consists in computing a fixed-time fuel optimal, finite sequence of impulsive maneuvers performed by the active spacecraft such that (one of) the risk reduction criteria above, as well as saturation and operational constraints, are met.

Even in this simplified and restricted theoretical framework, there are relatively few existing works like those of Duncan et al. (2011); Kotz et al. (2012), which are based on defining a penalty function as the sum between the objective function and a penalty parameter multiplied by a measure of violation of the constraints. The resulting non-constrained optimization problem is solved either with derivative-free methods or by evolutionary optimization methods.

In this work, we revisit and analyze several reformulations of the Collision Avoidance Maneuver (CAM) design problem, when considering short-term encounters, in a specific practical framework provided by the French Space Agency (CNES). By extending and adapting the methods of Slater et al. (2006), Bombardelli and Hernando-Ayuso (2015) and Armellin (2021), the formulation of nonconvex Quadratically Constrained Linear Programming (QCLP) problems is proposed in Section 2.

⋆ The Authors would like to thank CNES for its partial financial support of this work and Thales Alenia Space for giving access to realistic space data.

These are known to be NP-hard (Vavasis (1995)) as soon as more than one quadratic constraint is present, with few algorithms existing in the literature ((Floudas and Visweswaran, 1995, Sec. 8)). We focus in Section 3 on two distinct classes of numerical approaches composed each of two different methods. The first two methods rely on SemiDefinite Programming (SDP) as a common basis, with the first one exploiting recent results in semi-algebraic optimization, while the second one rather uses a randomization step. The second class consists of branch and bound (B&B) algorithms with set-based arithmetic (boxes or ellipsoids). On the one hand, the more sofisticated and mature approach of the IBEX software [1] is considered, which uses contractors (based on a filtering concept borrowed to constraint programming). On the other hand, a prototype experimental algorithm inspired by the ellipsoid method is investigated.

While lacking exhaustiveness, our choice of numerical approaches has a twofold motivation: firstly, we are interested in providing a stand-alone algorithm that can be directly included in existing CNES software tools; secondly, we considered both general well-established routines that converge towards global optimality and more ad-hoc procedures that are efficient on practical CNES examples. Therefore, in Section 4, we compare and evaluate these different approaches on realistic space and academic examples, using IBEX as the reference method because of its greater maturity.

Notations: $O_{p\times m}$ and $I_m$ denote respectively the null matrix of dimensions $p\times m$, the identity matrix of dimension $m$. $\mathbb{N}^n_d := \{\alpha\in\mathbb{N}^n : |\alpha|\leq d\}$, where $|\alpha| = \sum_i \alpha_i$ and $\alpha =$ is a multi-index. Indeed, $y_\alpha = y_1^{\alpha_1}\cdots y_n^{\alpha_n}$ with $|\alpha|\leq d$ and for $\alpha\in\mathbb{N}^n_d$. For a symmetric real matrix $S\in\mathbb{R}^{n\times n}$, the notation $S\preceq 0$ ($S\succeq 0$) stands for the negative (positive) semi-definiteness of $S$ while $u\preceq v$ means the component-wise inequality for the two vectors $u$ and $v$ of identical dimensions. For the random vector $\xi$, $\mathbb{E}(\xi)$ is its expectation. Finally, $\lceil a\rceil$ is the nearest integer greater than or equal to $a$. Finally, $\partial f$ is the subdifferential (set of subgradients) of the function $f$.

## 2. A GENERIC CAM DESIGN PROBLEM FORMULATED AS A LINEAR OPTIMIZATION PROBLEM WITH NON-CONVEX QUADRATIC CONSTRAINTS

The objective of this section is to propose a generic framework for CAM design taking into account station-keeping requirements, a variety of operational constraints and a great diversity of possible missions.

However, for the sake of practicality, we closely follow CNES operational procedures and insight, which lead to a specific CAM problem, defined as follows. Besides the low-thrust specific operational constraints mentioned in the introduction, we consider station-keeping requirements and also the necessity to reduce the impact of CAMs on mission service by forbidding attitude changes in the avoidance phase. Specifically, the primary is actuated by one or more impulsive CAMs that must take place over user-predefined time ranges $\Delta_i$, with $i=1,\cdots,n$. It is assumed that only the central date $t^i\in\Delta_i$ is allowed per maneuver in order to be able to perform an *a posteriori* spread of the thrust over the time ranges for an equivalent low-thrust propulsion. It is also assumed that only one identical thrust direction for all $\Delta_i$ is possible. More precisely, the thrust vector is defined at $t^i$ by $\Delta V_i^T = \Delta v_i \beta_l^T$, where $\Delta v_i$ is the magnitude of the impulse and $\beta_l$ is the $l$-th vector of the canonical basis in the local frame, where the index $l$ is set to 1, 2 or 3 for all $i=1,\cdots,n$ and $\Delta v_i\geq 0$. The magnitude of the thrusts is also bounded as $\Delta v_i\leq \Delta\bar{v}_i$.

Furthermore, the relative motion of each secondary object $s_j$, with $j=1,\ldots,N$, is described by a transition matrix obtained by a linearization of the Keplerian dynamics around the mean ballistic orbit of the primary (cf. Yamanaka and Ankersen (2002)):

$$x_{r_j}(t|x^0_{r_j}) = \Phi^j_r(t,t_0)x^0_{r_j}, \tag{1}$$

where $x^0_{r_j}$ denotes the initial relative state of the $j$-th object wrt. the primary and the transition matrix $\Phi^j_r$ is given by blocks as follows

$$\Phi^j_r(t,t_0) := \begin{pmatrix} \Phi^j_{r_{11}}(t,t_0) & \Phi^j_{r_{12}}(t,t_0) \\ \Phi^j_{r_{21}}(t,t_0) & \Phi^j_{r_{22}}(t,t_0)\end{pmatrix}.$$

Denoting $\tilde{x}_{r_j}$ the relative state of the $j$-th object with respect to the primary (after a maneuver), one has, after $n$ impulsive maneuvers in the $\beta_l$ direction, applied respectively at $t^i$ with a magnitude $\Delta v_i$:

$$\begin{aligned}\tilde{x}_{r_j}(t|t_0) &= x_{r_j}(t|t_0) + \sum_{i=1}^n \Phi^{lj}_r(t,t^i)\Delta v_i \\ &= \Phi^j_r(t,t_0)x^0_{r_j} + \sum_{i=1}^n \Phi^{lj}_r(t,t^i)\Delta v_i,\end{aligned} \tag{2}$$

where $\Phi^{lj}_r(t,t^i)$ is the $3+l$-th column of the matrix $\Phi^j_r(t,t^i)$. From Equation (2), it is straightforward to derive the relation between the uncontrolled (position $r_{r_j}$ and velocity $v_{r_j}$) and controlled (position $\tilde{r}_{r_j}$ and velocity $\tilde{v}_{r_j}$) relative states for each encounter at $t^j_{\mathrm{TCA}}$:

$$\tilde{r}_{r_j}(t^j_{\mathrm{TCA}}) = r_{r_j}(t^j_{\mathrm{TCA}}) + \sum_{i=1}^n \Phi^{lj}_{r_{12}}(t^j_{\mathrm{TCA}},t^i)\Delta v_i, \tag{3}$$

$$\tilde{v}_{r_j}(t^j_{\mathrm{TCA}}) = v_{r_j}(t^j_{\mathrm{TCA}}) + \sum_{i=1}^n \Phi^{lj}_{r_{22}}(t^j_{\mathrm{TCA}},t^i)\Delta v_i. \tag{4}$$

Equations (3) and (4) allow for the estimation of the miss distance, the Mahalanobis distance as well as the collision probability at each $t^j_{\mathrm{TCA}}$ to be used as metrics for the CAM triggering.

### 2.1 Miss distance metric formulation

Assuming a rectilinear uniform relative motion around $t^j_{\mathrm{TCA}}$ of directional unit vector:

$$e_j = \frac{\tilde{v}_{r_j}(t^j_{\mathrm{TCA}})}{\|\tilde{v}_{r_j}(t^j_{\mathrm{TCA}})\|}, \tag{5}$$

the new miss-distance $d^{\mathrm{new}}_j$ is given by the norm of the projection $\Delta r^j_{\min}$ of the vector $\tilde{r}_{r_j}(t^j_{\mathrm{TCA}})$ on the encounter B-plane orthogonal to $e_j$. Formally, this reads:

$$\Delta r^j_{\min} = (I_3 - e_j e_j^T)\tilde{r}_{r_j}(t^j_{\mathrm{TCA}}), \tag{6}$$

where $I_3 - e_j e_j^T$ is the (symmetric and idempotent) projection matrix on the $j$-th B-plane. One obtains:

$$\begin{aligned}d_j^{\mathrm{new}^2} &= r_{r_j}(t^j_{\mathrm{TCA}})^T(I_3 - e_j e_j^T)r_{r_j}(t^j_{\mathrm{TCA}}) \\ &+2r_{r_j}(t^j_{\mathrm{TCA}})^T(I_3 - e_j e_j^T)\tilde{\Phi}^{lj}_{r_{12}}\Delta v \\ &+\Delta v^T\tilde{\Phi}^{lj^T}_{r_{12}}(I_3 - e_j e_j^T)\tilde{\Phi}^{lj}_{r_{12}}\Delta v,\end{aligned} \tag{7}$$

[1] http://www.ibex-lib.org

where $\Delta v^T$ contains the magnitudes of the $n$ impulses:

$$\Delta v^T = [\,\Delta v_1,\ \Delta v_2,\ \cdots,\ \Delta v_n\,],$$

and similarly, $\tilde{\Phi}^{lj}_{r_{12}}$ is given by the concatenation of the columns $\Phi^l_{r_{12}}(t^j_{\text{TCA}}, t^i)$ for $i = 1, \cdots, n$.

Hence, $d_j^{\text{new}^2}$ is a convex quadratic form:

$$d_j^{\text{new}^2} := \Delta v^T Q_j \Delta v + 2q_j^T \Delta v + p_j, \tag{8}$$

where $Q_j, q_j, p_j$ are identified from Equation (7). Note that the matrices $Q_j$ are semidefinite positive ones and imposing a prescribed minimal miss distance threshold $\sqrt{\underline{d}_j}$ after the CAMs, at each $t^j_{\text{TCA}}$, defines a concave domain:

$$\Delta v^T Q_j \Delta v + 2q_j^T \Delta v + p_j \geq \underline{d}_j,\ j = 1, \cdots, N. \tag{9}$$

It turns out that the choice of the metric characterizing the collision (miss distance, Mahalanobis distance, 2D probability, maximum probability) has no direct influence on the nature of the obtained problem, since in all cases, the same class of problems is obtained *in fine*, when considering the same assumptions used in the multiple short-term encounters framework (see also Armellin (2021) for further details on different metrics) defined by CNES.

### *2.2 Linear constraints: Station-keeping and control bounds requirements*

The after-CAMs station-keeping requirements impose the primary to remain in a box defined with respect to the reference bounds on the relative positions for each direction in a local frame at each $t^j_{\text{TCA}}$. This generates a set of linear inequalities on the decision variables (the inequality sign is meant componentwise):

$$\underline{u}_r^j - r_{r_j}(t^j_{\text{TCA}}) \preceq \tilde{\Phi}^{lj}_{r_{12}} \Delta v \preceq \overline{u}_r^j - r_{r_j}(t^j_{\text{TCA}}),\ j = 1, \cdots, N, \tag{10}$$

for user set bounds $\underline{u}_r^j$ and $\overline{u}_r^j$. Similarly, another set of linear inequalities on the decision variables is added due to bounds on the magnitude of the impulsive thrusts:

$$0_{n\times 1} \preceq \Delta v \preceq \Delta \overline{v}. \tag{11}$$

Finally, our goal is to minimize the impact of the CAMs on the satellite lifetime and so, the minimum-fuel multi-risk collision avoidance problem is formulated as a non-convex quadratically constrained optimization problem with a linear objective:

$$\begin{aligned} \min_{\Delta v \in \mathbb{R}^n}\ & c^T \Delta v \\ \text{s.t.}\ & \Delta v^T Q_j \Delta v + q_j^T \Delta v + p_j \geq \underline{d}_j,\ j = 1, \cdots, N, \\ & A\Delta v \preceq b, \\ & \Delta v \succeq 0_{n\times 1} \end{aligned} \tag{12}$$

where $c^T = [\,1,\ 1,\ \cdots,\ 1\,] \in \mathbb{R}^n$, and $Q_j$, $q_j$, $p_j$, $A$ and $b$ are identified from Equations (9), (10), (11). The optimization problem (12) consists in minimizing a linear function on a domain given by the intersection between the polyhedron defined by the linear inequalities and the non-convex domain defined by the exterior of a union of (possibly degenerate) ellipsoids. The feasible domain of this optimization problem is therefore non-convex (and possibly non-connected in some cases).

## 3. NUMERICAL ALGORITHMS

As already mentioned, Problem (12) is a special case of non-convex QCLP problems, for which two classes of algorithms (based either on SDP or B&B with set-valued arithmetic) are to be summarized and then compared on numerical examples in the next section. Starting with the first category, note that Problem (12) is a polynomial optimization problem of the form:

$$\begin{aligned} f^* = \inf_{x\in\mathbb{R}^n}\ & f(x), \\ \text{s.t. } & g_\ell(x) \geq 0, \ell = 1, \ldots, r, \end{aligned} \tag{13}$$

where $f$ and $g_\ell$ are multivariate polynomials (or affine functions). Let $\mathbf{K}$ denote the feasible set of (13).

### *3.1 A moment-SOS hierarchy of SDP relaxations*

Lasserre's hierarchy (Lasserre (2015)) is a well-known method to approximate the optimal value of such problems based on semidefinite programming (SDP). From a computational viewpoint, a hierarchy of SDP problems is solved, which provides lower bounds that are convergent to the optimal value of the original problem. However, for large scale problems, the size of the involved SDP may be prohibitive, as well as the numerical extraction of the corresponding optimizers. In (Lasserre, 2015, Section 5.1), it is shown that:

$$\begin{aligned} f^* = \inf_{\nu\in\mathbb{M}(\mathbf{K})_+}\ & \int_{\mathbf{K}} f \mathrm{d}\nu \\ \text{s.t.}\ & \nu(\mathbf{K}) = 1, \end{aligned} \tag{14}$$

where $\mathbb{M}(\mathbf{K})_+$ is the space of finite nonnegative Borel measures on $\mathbf{K}$. The Problem (14) is a linear programming problem in an infinite-dimensional space and as such, it is difficult to get a direct solution in terms of the decision variable $\nu$ which is an unknown measure. However, this unknown measure $\nu$ may be represented by the infinite sequence of its moments $y_\alpha = \int_{\mathbf{K}} x^\alpha \mathrm{d}\nu,\ \forall\ \alpha \in \mathbb{N}^n_d$ and the Problem (14) may be recast as:

$$f^* = \inf_y \left\{ \sum_{\alpha\in\mathbb{N}^n_d} f_\alpha y_\alpha\ :\ \exists\ \nu \in \mathbb{M}(\mathbf{K})_+ \text{ s.t. } y_0 = 1 \right\}.$$

Thanks to strong results obtained in the framework of the (real) K-moment problem (i.e. constructing the sequences $(y_\alpha)$ that are moment sequences of a nonnegative measure $\nu$ with its support contained in set $\mathbf{K}$) for a compact basic semi-algebraic set $\mathbf{K}$ (see (Lasserre, 2015, Section 2.7.2 and Section 2.7.3) for technical details), a hierarchy of semidefinite relaxations of Problem (13) may be defined as the following:

$$\begin{aligned} f_d^* = \inf_y\ & L_y(c^T x) \\ & M_d(y) \succeq 0 \\ \text{s.t.}\ & M_{d-\varsigma_\ell}(g_\ell y) \succeq 0,\ \ell = 1, \cdots, r \\ & y_0 = 1, \end{aligned} \tag{15}$$

where $g_0 = 1$, $\varsigma_\ell = \lceil (\deg(g_\ell))/2 \rceil$, $\ell = 0, \cdots, r$, $d \geq d_0 = \max\{\lceil (\deg(f))/2 \rceil,\ \max_{\ell=0,\cdots,r} \varsigma_\ell\}$. $L_y$ is the Riesz linear functional, $M_d(y)$ is the moment matrix and $M_{d-\varsigma_\ell}(g_\ell y)$ is the localizing matrix with respect to $y$ and $g_\ell$ (Lasserre, 2015, Section 2.7). Obviously, $f_d^* \leq f^*$ and $f_d^* \leq f_{d+1}^*$ for all $d$ since the set of constraints for order $d+1$ is included in the one for $d$. One of the main features of this hierarchy of relaxations lies in the finite convergence (a finite order $d$ exists s.t. $f_d^* = f^*$) of the hierarchy of semidefinite relaxations (15) under some classical conditions in nonlinear programming (strict complementarity condition, constraint qualification sufficient conditions, second-order sufficient condition of optimality). Under these conditions, this finite convergence result and a certificate of global optimality are mainly entailed by Putinar's Positivstellensatz and a technical assumption on the polynomials defining the

set $\mathbf{K}$, which is fulfilled in our case due to the compactness of $\mathbf{K}$. The algorithm based on the moments hierarchy is now summarized below.

**Algorithm 1** A HIERARCHY OF SDP RELAXATIONS

**Require:** Cost function $c$, set $\mathbf{K}$ defined by quadratic and linear constraints $g_\ell$, $\ell = 1, \cdots, r$, maximum order of the relaxation $\bar{d}$.

**Ensure:** Optimal cost $f^*$ and global minimizer $x^*$ of Problem (13) or lower bound $f_d^*$ of $f^*$.

▷ *Solution of SDP problem associated to relaxation of order d*
Solve the SDP Problem (15) to get $f_d^*$ and $y_d^*$ if it exists;
**if** $y_d^*$ does not exist **then**
  $f_d^*$ is only a lower bound of the optimum: $f_d^* \leq f^*$;
**else if** $d < \bar{d}$ **then**
  $d \leftarrow d+1$;
  Goto 1;
**end if**
▷ *Global optimality test*
**if** $\text{rank}(M_{d-\varsigma}(y_d^*)) = \text{rank}(M_d(y_d^*)) = k$ with $\varsigma = \max_\ell \varsigma_\ell$ **then**
  $f_d^* = f^*$ and $\exists$ at least $\text{rank}(M_d(y_d^*)) = k$ global minimizers $y^*$ that may be extracted.
**end if**
**if** $(\text{rank}(M_{d-\varsigma}(y_d^*)) \neq \text{rank}(M_d(y_d^*)))$ and $(d < \bar{d})$ **then**
  $d \leftarrow d+1$;
  Goto 1;
**else**
  Stop. $f_d^*$ is only a lower bound of the optimum: $f_d^* \leq f^*$.
**end if**

### *3.2 Semidefinite relaxation and randomization approach*

A straightforward convex relaxation of the Problem (12) may also be derived by adding decision variables allowing to linearize the problem as follows (Luo et al. (2010)). Let $X$ denote a $n \times n$ symmetric matrix, then the Problem (12) can be written as:

$$\begin{aligned} \min_{x,X} \; & c^T x \\ \text{s.t.} \; & \begin{aligned} \text{trace}(Q_j X) + q_j^T x + p_j &\geq 0, \; j = 1, \cdots, N, \\ Ax &\preceq b, \\ x &\succeq 0, \\ X - xx^T &= 0. \end{aligned} \end{aligned} \tag{16}$$

The last equality constraint $X - xx^T$, in which the non convexity of the problem is aggregated, is now replaced with a convex constraint $X - xx^T \succeq 0_{n\times n}$ leading to the SDP relaxation:

$$\begin{aligned} f_{\text{sdp}}^* = \min_{x,X} \; & c^T x \\ \text{s.t.} \; & \begin{aligned} \text{trace}(Q_j X) + q_j^T x + p_j &\geq 0, \; j = 1, \cdots, N, \\ Ax &\preceq b, \\ x &\succeq 0, \\ \begin{bmatrix} 1 & x^T \\ x & X \end{bmatrix} &\succeq 0, \end{aligned} \end{aligned} \tag{17}$$

after using a Schur complement argument on the last constraint. This derivation may be considered as a particular instance of a lifting technique. Note also that (17) is the Lagrangian bidual of the nonconvex original problem. In addition, the relaxation (17) is exactly the relaxation (15) of (13) for $d = 1$. As a convex relaxation, the Problem (17) provides in general only a lower bound of the optimal solution of the genuine nonconvex Problem (12). Moreover, an optimal pair $(X^*, \bar{x}^*)$ solution of (17) may not be feasible for the Problem (16) and $x^*$ cannot be used in general as a solution of (12). However, a simple stochastic interpretation of the pair $(X^*, \bar{x}^*)$ will help in finding a systematic way to generate samples in the feasible set of (12). Then, the best sampled feasible point provides a good approximation $x_{srr}^*$ of the optimal solution of (12). Indeed, for an optimal pair $(X^*, \bar{x}^*)$ solution of (17), the matrix $X - \bar{x}\bar{x}^T$ is a covariance matrix. Then, by defining the random vector $\xi$ distributed as the normal vector $\xi \sim \mathcal{N}(\mu = \bar{x}^*, \Sigma = X^* - \bar{x}^*\bar{x}^{*T})$, it is simple to show that $(\mu, \Sigma)$ is a pair solution of the following stochastic programming problem.

$$\begin{aligned} \min_{\mu,\Sigma} \; & \mathbb{E}(\xi) = c^T \mu \\ \text{s.t.} \; & \begin{aligned} \mathbb{E}(g_j(\xi)) &\geq 0, \; j = 1, \cdots, N, \\ \mathbb{E}(A\xi) = A\mu &\preceq b, \\ \mathbb{E}(\xi) = \mu &\succeq 0, \\ \Sigma &\succeq 0. \end{aligned} \end{aligned} \tag{18}$$

where $\mathbb{E}(\cdot)$ is the expectation operator. Loosely speaking, $\xi$ is an "average" solution of (12) over the Gaussian distribution, meaning that the expected value of the objective is minimized and the constraints are satisfied in expectation. This interpretation provides a procedure to build a representative sampling of the feasible set of (13). It consists in drawing $L$ samples $\hat{\xi}(i)$ from the truncated $(0 \preceq \hat{\xi}(i) \preceq \Delta\bar{v})$ Gaussian distribution $\xi \sim \mathcal{N}(\mu, \Sigma)$. If the sample $\hat{\xi}(i)$ does not satisfy the constraints in (12), project it onto the feasible set $\mathbf{K}$ as $\bar{\xi}(i)$. This procedure is now detailed in the Algorithm 2 given below.

**Algorithm 2** $\text{SRR}(c, Q_j, q_j, p_j, A, B)$

**Require:** Cost vector $c$, matrices $Q_j$, $j = 1, \cdots, N$, $A$, vectors $q_j$, $j = 1, \cdots, N$, $b$, points $p_j$, $j = 1, \cdots, N$.

**Ensure:** Approximation $x_{srr}^*$ of the optimal solution of Problem (13).

Solve of SDP relaxation (17) to get $\bar{x}^*$ et $X^*$ ;
▷ *Feasibility test of the solution of the relaxation*
**if** $\bar{x}^* \in \mathbf{K}$ **then**
  $x^* \leftarrow \bar{x}^*$ ; Stop ;
**else**
  Draw L samples $\hat{\xi}(i)$, $i = 1, \cdots, L$ from the multivariate Gaussian $\mathcal{N}(\bar{x}^*, X^* - x^* x^{*T})$ tuncated in the set $\{0 \preceq x \preceq \Delta\bar{v}\}$ ;
  ▷ *Feasibility test of the samples*
  **for** $i \leftarrow 1$ to $L$ **do**
    **if** $\hat{\xi}(i) \in \mathbf{K}$ **then**
      $x(i) \leftarrow \hat{\xi}(i)$ ;
    **else**
      **for** $j \leftarrow 1$ to $N$ **do**
        Compute $val(j) = \left[ \hat{\xi}(i) + 0.5 * Q_i * q_i \right]^T * Q_j^{-1} * (\frac{q_j^T Q_j^{-1} q_j}{4} - p_j)^{-1} * \left[ \hat{\xi}(i) + 0.5 * Q_i * q_i \right]$ ;
      **end for**
      $val_{min} \leftarrow \min_{j=1,\cdots,N} val$ ; $jmin \leftarrow \arg\left[ \min_{j=1,\cdots,N} val \right]$ ;
      **if** $val_{min} < 1$ **then**
        $\bar{\xi}(i) = ((\hat{\xi}(i) + 0.5 * Q_{jmin} * q_{jmin}) / \sqrt{val_{min}}) - 0.5 * Q_{jmin} * q_{jmin}$ ;
      **end if**
      ▷ *Feasibility test of the scaled sample* $\bar{\xi}(i)$ *in* $\mathbf{K}$
      **if** $\bar{\xi}(i) \in \mathbf{K}$ **then**
        $x(i) \leftarrow \bar{\xi}(i)$ ;
      **end if**
    **end if**
  **end for**
  $x_{srr}^* \leftarrow \arg\left[ \min_i c^T x(i) \right]$ ;
**end if**

### 3.3 B&B algorithms with set-based arithmetic

An alternative classical approach to problem (12) is based on subsequent subdivision of an initial search domain (defined in the space of decision variables and including the initial feasible domain), via B&B algorithms. At each iteration, one discards subdomains found to be infeasible or subdomains whose minimum attained objective value (by any of its feasible points) is greater than the current best objective value found so far by the algorithm. The subdivision process stops for a subdomain when the difference between a lower bound and an upper bound of the objective function over the subregion is less than a given tolerance. The list of remaining subdomains contains all the optimal solutions. The main challenge lies in obtaining good lower and upper bounds of the objective function in a given subregion. A solution consists in representing the domains by boxes (axes-aligned interval tensors in $\mathbb{R}^n$) and evaluating the involved functions by interval analysis (see Fernández and Boglárka (2022) for a recent review of interval branch-and-bound based methods for global optimization).

**IBEX Software.** For instance, Ninin (2015) describes Ibex implementation with constraint propagation techniques suitable for constrained global optimization problems. To accelerate convergence, contractors are used at each iteration to prune the width of boxes. Inspired by the filtering concept in constraint programming, the goal of a contractor is to eliminate unfeasible parts of a domain. For instance, some contractors of IBEX (which are used by default) are based on linear relaxation: given a system of linear inequalities, a box is contracted to the hull of the polytope (the set of feasible points); non-linear constraints are automatically linearized by Taylor or affine arithmetic. Also, constraint propagation algorithm HC4 and shaving contractors (which aim at elliminating a slice of a box by calling a contractor on it) are used by default. Ninin (2015) mentions that the performance of the default optimizer is comparable to the global optimizer BARON, while also performing all the operations in a set-based arithmetic, which ensures that no solution is lost. As it will be shown in Section 4, this performance claim is confirmed on the tests specific to our problem.

**Ellipsoid-based B&B.** Since our specific problem is the QCLP-type, a natural set-based extension of interval algorithms is to represent the underlying subdomains by ellipsoids. Starting from an ellipsoid containing the initial feasible domain, the idea is to generate a sequence of ellipsoids of smaller volumes by employing cutting planes, like in the classical ellipsoid algorithm of Yudin and Nemirovski (see Bland et al. (1981) for a detailed historical and technical description).

More precisely, the minimization of a convex function $f : \mathbb{R}^n \to \mathbb{R}$, on an elliptic domain $\varepsilon_0 = \{x \in \mathbb{R}^n : (x-x_0)'P_0(x-x_0) \leq 1\}$, given a semidefinite positive matrix $P_0 \in \mathbb{R}^{n\times n}$ consists in the convergent iteration (starting with $k = 0$) of the following two steps:

- *Calculate a sub-gradient $h_k \in \partial f(x_k)$ at the center $x_k$ of the ellipsoid, which allows for identifying a cutting plane and thus a half-space containing $x_k$ but no minimizer of $f$;*
- *Calculate and return the ellipsoid $\varepsilon_{k+1}$ of minimal volume containing the half-ellipsoid $\varepsilon_k \cap \{x \in \mathbb{R}^n : h_k^T(x-x_k) \leq 0\}$ which contains a minimizer of $f$.*

This procedure, called in what follows ELLIPSOIDCUT can be easily modified to reduce the volume of an ellipsoid wrt. convex-constraints: when no reduction is possible, either the center is feasible, or the ellipsoid is completely empty.

As expected, since our problem is not convex, a subdivision strategy is necessary: an ellipsoid is bisected by a cutting plane (as above) function of its longest axis. The resulting Algorithm 3 keeps track of a list of ellipsoids which are guaranteed to contain all the optimal solutions.

**Algorithm 3** BRANCHANDBOUNDELLIPSOID

**Require:** Initial quadratic domain $(x-o_0)'P_0(x-o_0) \leq 1$, Nonconvex Quadratic constraints ELLIPSOIDSLIST, Linear constraints LINEARCONSTRLIST, linear objective $c$, subdivision accuracy $\varepsilon_{\text{VMin}}$.

**Ensure:** Minimal cost $c_m$, value $o_m$ and list of ellipsoids containing all the global optimizers $L_{keep}$.

```
▷ Start with initial ellipsoid
L ← ∅; Push (L,(P_0,o_0)), c_m ← +∞
while L ≠ ∅ do
  (P,o) ←Pop(L)
  if VOLUMEELLIPSOID(P) ≤ ε_VMin then
    Push(L_keep,(P,o))
  else
    ▷ Volume contractor wrt. linear constraints
    (P,o) ←ELLIPSOIDCUT((P,o),LINEARCONSTRLIST)
    if (P,o) ≠ ∅ then
      ▷ Test center feasibility wrt. non-convex constraints
      if ISFEASIBLE(o,ELLIPSOIDLIST) then
        {Update current minimum}
        if c_m > c^T o then
          c_m ← c^T o; o_m ← o
        end if
        ▷ Volume contractor wrt. objective
        (P,o) ←ELLIPSOIDCUT((P,o),c)
        Push((P,o),L)
      else
        ▷ Subdivide ellipsoid
        (P_1,o_1,P_2,o_2) ← BISECTELLIPSOID(P,o)
        Push((P_1,o_1),(P_2,o_2),L)
      end if
    end if
  end if
end while
return (c_m,o_m)
```

## 4. NUMERICAL EXAMPLES

Prototype implementations of the three algorithms were initially [2] coded and tested in Matlab© R2020b. For completeness' sake, we have also included results obtained with the IBEX Optimization tool (with default parameters). Timings are provided, but since this implementation is in C++, a performance comparison is difficult to make.

First, in Section 4, two numerical examples with a limited number of conjunctions (from 1 to 3) and two maneuvers are built by using real space data. Even though the proposed numerical examples are not based on real conjunction data, two realistic operational situations are proposed by considering an actual telecom satellite as a model for the definition of the primary object.

Secondly, the efficiency and scalability of the algorithms are tested on some random academic examples of nonconvex quadratic problems (13). These tests still focus only on some

[2] A more efficient implementation is available in CNES flight dynamics Java library PATRIUS.

expected maximum realistic operational situations: up to 8 maneuvers and less than 20 conjunctions. The details of the design of this set of random examples are given in Subsection 4.2.

### *4.1 Two realistic examples with 2 maneuvers*

This section describes the common framework used for building two realistic encounter geometries presented in the following subsections. Specific details pertaining to a given test case, e.g. TCAs, maneuvers times or station-keeping constraints, are given in later subsections. The full orbital elements set of the model for the primary object is given in Table 1.

| | |
|---|---|
| Semi-major axis | $a = 7158$ km |
| Inclination | $i = 86.4$ deg. |
| Argument of Perigee | $\omega = 0$ deg. |
| RAAN | $\Omega = 0$ deg. |
| Eccentricity | $e = 0.00145$ |
| True Anomaly | $v_0 = 90$ deg. |

Table 1. Orbital parameters of the primary object.

In order to set up the orbits of the secondaries, the orbit of the primary is propagated from the epoch to the TCA corresponding to the associated conjunction. The relative positions and velocities at this TCA are added to the position and velocity of this propagated orbit, creating the cartesian orbit of the associated secondary. The relative positions and velocities in the NTW frame (as it is defined in (Vallado, 2001, Section 3.3.3)) are given in Table 2 for the three secondaries considered in the following. This table contains additional data consisting in the miss-distance for each possible conjunction, the semi-major axis and inclination of each secondary. Even if the algorithms

| | CDM 1 | CDM 2 | CDM 3 |
|---|---|---|---|
| Rel. pos. (m) | $\begin{bmatrix} -7.9 \\ 35 \\ 80 \end{bmatrix}$ | $\begin{bmatrix} -16.8 \\ -1.8 \\ 41 \end{bmatrix}$ | $\begin{bmatrix} 0.9 \\ -35.2 \\ -3 \end{bmatrix}$ |
| Rel. vel. (m/s) | $\begin{bmatrix} 5.7 \\ -12552.6 \\ 5489 \end{bmatrix}$ | $\begin{bmatrix} -38 \\ -14910.8 \\ -785.5 \end{bmatrix}$ | $\begin{bmatrix} 0.6 \\ -0.5 \\ 5.8 \end{bmatrix}$ |
| Miss dist. (m) | 87 | 44 | 35 |
| a (km) | 7120 | 7147 | 6902 |
| i (deg.) | 98.4 | 98.4 | 97.5 |

Table 2. Data for the secondaries orbits.

are not limited to two maneuvers, we chose to stick to two maneuvers, allowing a simple graphical illustration in the $\Delta v_1$, $\Delta v_2$ plane of both the feasible domain and the optimal solution. For each numerical example, the two impulsive maneuvers are given along one single direction of the local NTW frame as detailed in Section 2. For each example, the parameters of the three algorithms are the same: $\varepsilon_{\text{vol.}} = 0.0001$ for the ellipsoidal B. and B. algorithm, 5000 draws for the SDR method and relaxation of order 2 for the moment relaxation approach.

*Test case 1: two impulsive maneuvers in the T direction and 1 TCA.* The first example is essentially designed to be a proof-of-concept example for the different algorithms proposed. Therefore, only one risk (a single secondary) corresponding to CDM 2 in Table 2 is considered with a TCA given at $t_0 + 24$ h.. The two maneuvers are respectively set to TCA minus 1 orbit ($t_0$+22.33 h.) and TCA minus 0.5 orbit ($t_0$+23.16 h.) and are in the Tangential direction (T) with a limit in magnitude of 15 m/s for each thrust. The station-keeping box on the positions and velocities of the primary is defined in the RTN (Radial, Transverse and Normal) or Gaussian coordinate system (see (Vallado, 2001, Section 3.3.3)) by the vector $[\,5\ 6\ 5\,]$ km for the positions and $[\,10\ 10\ 10\,]$ m/s for the velocities.

| | $\Delta v_1$ (m/s) | $\Delta v_2$ (m/s) | CPU time (s) | Obj. (m/s) |
|---|---|---|---|---|
| IBEX | 0.0285 | 0 | 1 | 0.0285 |
| Elli. B. & B. | 0.0333 | 0.0002 | 1.26 | 0.0335 |
| SRR | 0.0285 | 0 | 6.5 | 0.0285 |
| Moment relax. | 0.0285 | 0 | 3.3 | 0.0285 |

Table 3. Results of the different algorithms for Example 1.

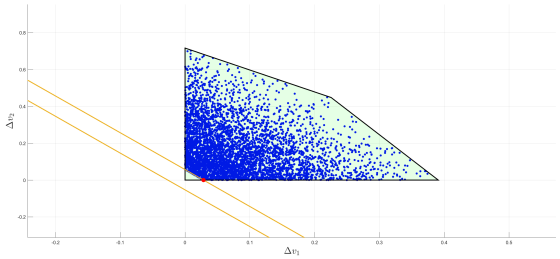

Figure 1. Polytopic feasible region (light green with black edges), one quadratic constraint (yellow ellipse), optimal solution (red point) and feasible solutions (blue points).

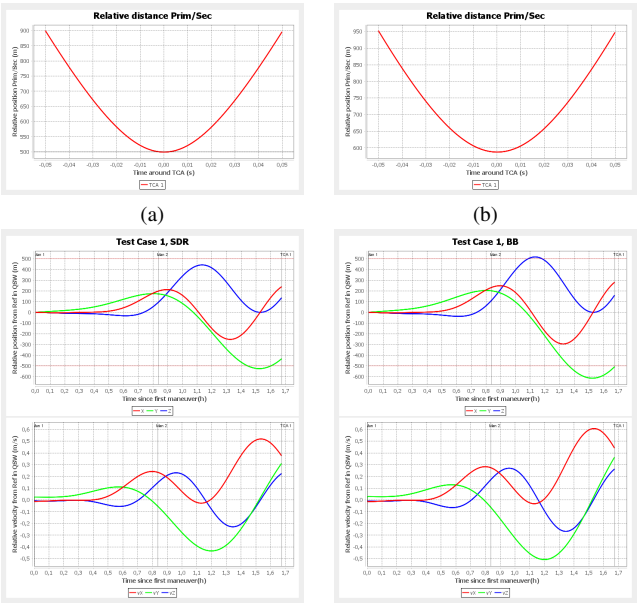


(a) (b) (c) (d)

Table 4. (a) and (b) Miss distance (m.) around TCA for SRR algorithm and BB algorithm (c) and (d) Relative positions and velocities trajectories from MAP reference in QSW frame for SRR and BB maneuvers.

The obtained results are summarized in Table 3 while Figure 1 exhibits the geometry of the nonconvex quadratic optimization problem in the decision variables plane as well as the behavior of the SRR algorithm. It is easily seen in Table 3 that all algorithms perform well in finding the global optimal solution in a reasonable timing except for the ellispoidal B&B algorithm which gives, though very quickly, a worst quality approximation of the optimal solution. This could be fixed by choosing a more accurate precision parameter $\varepsilon_{\text{vol.}}$ (0.000001 would be

sufficient here) at the expense of a slight rise of the CPU time. It is worth noticing that the relative trajectories presented in Figure 4 comply with the restrictions in all cases even if the deviation from the reference is more important in the case of the approximate optimal solution given by the ellipsoidal B&B algorithm.

*Test case 2: Two impulsive maneuvers in the N direction and 3 TCAs.* For this second example, a sequence of three short-term close approaches between the primary and three secondaries (characterized by the 3 CDMs provided by CNES and given in Table 2) are defined. The three TCAs are respectively set at $t_0$ + 24 h., $t_0$+25.5 h. and $t_0$+34 h.. The two maneuvers are respectively set to TCA1 minus 1.5 orbit ($t_0$+21.58 h.) and TCA1 minus 1 orbit ($t_0$+22.39 h.) and are in the Normal direction (N) with a limit in magnitude of 15 m/s for each thrust. The station-keeping box on the positions and velocities of the primary is defined in the RTN by the vector $[\,1\ \ 5\ \ 6\,]$ km for the positions and $[\,10\ \ 10\ \ 10\,]$ m/s for the velocities. The obtained results are summarized in Table 5, while Figure 2 exhibits the geometry of the nonconvex quadratic optimization problem in the decision variables plane as well as the behavior of the SRR algorithm. Identical conclusions may be drawn from the reading of Table 5 with an additional difficulty for the ellipsoidal B&B algorithm when the number of nonconvex quadratic constraints increases. This feature will be more prominent when dealing with academic examples with a more important number of decision variables and nonconvex constraints. In this particular case, the worst quality approximaton of B&B algorithm does not have a significant impact on the relative trajectories.

| | $\Delta v_1$ (m/s) | $\Delta v_2$ (m/s) | CPU time (s) | Obj. (m/s) |
|---|---|---|---|---|
| IBEX | 0.2455 | 0.2255 | 1 | 0.4710 |
| Elli. B. & C. | 0.2469 | 0.2323 | 13.8 | 0.4792 |
| SRR | 0.2455 | 0.2259 | 1.97 | 0.4714 |
| Moment relax. | 0.2455 | 0.2255 | 4.11 | 0.4710 |

Table 5. Results of the different algorithms for Example 2.

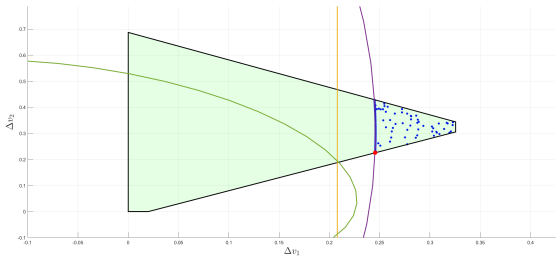

Figure 2. Polytopic feasible region (light green), three quadratic constraints (yellow, green and purple), optimal solution (red) and feasible solutions (blue).

### 4.2 *Other examples with $n > 2$*

For a fixed number $n$ of decision variables, $N$ quadratic constraints are randomly generated in this $n$-dimensional space. The $N-1$ ellipsoid centers are drawn from a uniform distribution on the interval $[-2,2]$ while the last quadratic constraint is an $n$-dimensional ball centered in 0 and of radius equal to 0.5. Finally, linear constraints $0 \leq x_i \leq \bar{x}_i$, for $i = 1, \cdots, n$ with $\bar{x}_i$ uniformly distributed in the interval $[1,3]$ are added to the quadratic constraints. Similar to the previously presented tests,

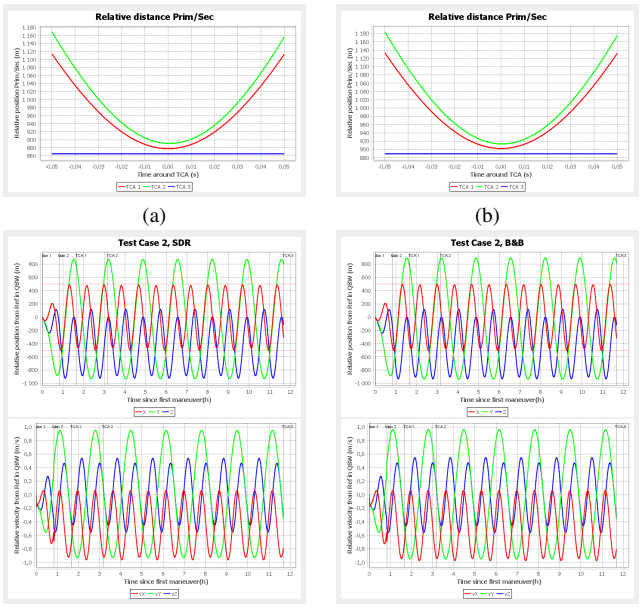


(a) (b) (c) (d)

Table 6. (a) and (b) Miss distance (m.) around TCA for SRR algorithm and BB algorithm (c) and (d) Relative positions and velocities trajectories from MAP reference in QSW frame for SRR and BB maneuvers.

$n$ corresponds to the number of maneuvers and respectively $N$ quantifies the number of conjunctions. Their maximum values are set to 8 and respectively 17, with the goal of providing an insight about the expected computational efficiency and accuracy for some more involved operational examples.

Table 7 provides a synthetic overview of timings and accuracy obtained with IBEX (C++ implementation, IbexOpt version 2.8, with default parameters). It follows that for these cases, this approach is very efficient, while providing set enclosures of the optimal value.

The results obtained with the other previously presented methods (prototyped and tested with Matlab© R2020b and the Mosek optimization toolbox (version 10) software for SDP solving) are summarized in Tables 8, 9 and 10. While for low-dimensional examples, the results are very similar, when the dimension increases, the reference software IBEX is clearly more efficient. Among the prototype algorithms, the SRR method provides the fastest results, at the expense of loosing theoretical guarantees of optimality.

It is interesting to note that the B&B methods seem to perform better on these particular instances. While being preliminary, this study of computational feasibility for a practical CNES problem reveals a potential lack of numerical efficiency for the first class of SDP-based implementations. Similarly, it goes to show that the interesting theoretical properties of the ellipsoid method need to be further tuned in order to be as efficient as the more mature interval boxes representation of set-based numerics.

## 5. CONCLUSION

While several works already dealt with the optimal collision avoidance for one short-term encounter (Bombardelli and Hernando-Ayuso (2015)), which can be solved by efficient convex optimization methods, the case of multiple short-term

| Case # | Solution features | | | | |
|---|---|---|---|---|---|
| | $n$ | $N$ | CPU (s) | $f_d^*$ | $f_{IBEX}^*$ |
| 3D | 3 | 17 | 0.05 | 0.5402 | 0.5414 |
| 4D | 4 | 10 | 0.12 | 0.5 | 0.5 |
| 5D | 5 | 10 | 0.23 | 1.42 | 1.4155 |
| 8D | 8 | 2 | 0.22 | 3.1632 | 3.1697 |

Table 7. IBEX results for higher-dimensional examples.

| Case # | Solution features | | | | | |
|---|---|---|---|---|---|---|
| | $n$ | $N$ | $L$ | CPU (s) | $f_d^*$ | $f_{SRR}^*$ |
| 3D | 3 | 17 | $10^4$ | 5.15 | 0.5402 | 0.5667 |
| 4D | 4 | 10 | $10^5$ | 4.03 | 0.5 | 0.5732 |
| 5D | 5 | 10 | $10^5$ | 4.8 | 1.142 | 1.7956 |
| 8D | 8 | 2 | $10^6$ | 11173 | 3.1623 | 5.77 |

Table 8. SRR results for higher-dimensional examples ($L$ corresponds to the number of random samples).

| Case # | Solution features | | | | |
|---|---|---|---|---|---|
| | $n$ | $N$ | $d$ | CPU (s) | $f_d^*$ |
| 3D | 1 | 17 | 4 | 2.12 | 0.5402 |
| 4D | 1 | 10 | 4 | 4.76 | 0.5 |
| 5D | 1 | 10 | 4 | 17.64 | 1.142 |
| 8D | 1 | 2 | 4 | 1633.5 | 3.1623 |

Table 9. Lasserre's hierarchy results for higher-dimensional examples ($d$ corresponds to the relaxation degree) .

| Case # | Solution features | | | | | |
|---|---|---|---|---|---|---|
| | $n$ | $N$ | $\varepsilon_{\text{VMin}}$ | CPU (s) | $f_d^*$ | $f_{\text{ell}}^*$ |
| 3D | 3 | 17 | 0.004 | 10.52 | 0.5402 | 0.74 |
| 3D | 3 | 17 | 0.0004 | 196.33 | 0.5402 | 0.59 |
| 4D | 4 | 10 | 0.0004 | 5.45 | 0.5 | 0.61 |
| 4D | 4 | 10 | 0.00004 | 171.6 | 0.5 | 0.54 |
| 5D | 5 | 5 | 0.004 | 0.4 | 1.142 | 2.55 |
| 5D | 5 | 5 | 0.0004 | 2.08 | 1.142 | 1.91 |
| 5D | 5 | 5 | 0.00004 | 55.15 | 1.142 | 1.72 |
| 8D | 8 | 2 | 0.0004 | 6181.3 | 3.16323 | 4.19 |

Table 10. Ellipsoid B&B results for higher-dimensional examples ($\varepsilon_{\text{VMin}}$ is the volume threshold for processed elliposids).

encounters boils down to a difficult non-convex NP-hard optimization problem. We formulated these problems by exploring the practical simplifications provided by CNES and observed that the indicator characterizing the collision (miss distance, Mahalanobis distance, 2D probability, maximum probability) has no direct influence on the QCLP nature of the problem obtained. As soon as at least two encounters are considered, the maneuver design is formulated as an optimization problem with linear objective and nonconvex quadratic constraints. The QCLP class of problems is then solved with several existing numerical methods whose efficiency is analyzed on realistic space examples and more academic and complex examples. These preliminary numerical analysis clearly show that the IBEX implementation is presently the most suitable and efficient tool to tackle the specific academic and realistic space examples dealt with in this article. Nevertheless, it is important to notice that the maturity of the implementation of the alternative tools based on SDP is not in any way comparable to the one of IBEX. A precise analysis of the impact of this implementation would definitely be an interesting future direction of research.

## REFERENCES


Armellin, R. (2021). Collision avoidance maneuver optimization with a multiple-impulse convex formulation. *Acta Astronautica*, 186, 347–362.

Bland, R., Goldfarb, D., and Todd, M. (1981). The ellipsoid method: A survey. *Operations research*, 29(6), 1039–1091.

Bombardelli, C. and Hernando-Ayuso, J. (2015). Optimal impulsive collision avoidance in low Earth orbit. *JGCD*, 38(2), 217–225.

Duncan, M., Wysack, J., and Wainwright, B. (2011). Optimal collision avoidance for multiple conjunction events. In *Proceedings of the AAS-AIAA Conference, Gridwood, Alaska, USA*.

Fernández, J. and Boglárka, G.T. (2022). Interval tools in branch-and-bound methods for global optimization. In S. Salhi and J. Boylan (eds.), *The Palgrave Handbook of Operations Research*, 237–267. Springer International Publishing, Cham.

Fernández-Mellado, L.S. and Vasile, M. (2021). On the use of machine learning and evidence theory to improve collision risk management. *Acta Astronautica*, 181, 694–706.

Floudas, C. and Visweswaran, V. (1995). Quadratic optimization. In *Handbook of global optimization*, volume 2, chapter 5, 217–269. Kluwer Academic Publishers.

Hennes, D., Izzo, D., and Landau, D. (2016). Fast approximators for optimal low-thrust hops between main belt asteroids. In *IEEE Symposium Series on Computational Intelligence*, 1–7.

Kotz, S., Johnson, N., and Boyd, D. (2012). A study on the collision avoidance maneuver optimization with multiple space debris. *Journal of Astronautical Sciences*, 1, 11–21.

Lasserre, J. (2015). *An Introduction to Polynomial and Semi-Algebraic Optimization*. Cambridge University Press.

Luo, Z.Q., Ma, W.K., So, A.C., Ye, Y., and Zhang, S. (2010). Semidefinite relaxation of quadratic optimization problems. *IEEE Signal Processing Magazine*, 27(3), 20–34.

Ninin, J. (2015). Global optimization based on contractor programming: An overview of the ibex library. In *International Conference on Mathematical Aspects of Computer and Information Sciences*, 555–559. Springer.

Slater, G., Byram, S., and Williams, T. (2006). Collision Avoidance for Satellites in Formation Flight. *JGCD*, 29(5), 1140–1146.

Vallado, D. (2001). *Fundamentals of astrodynamics and applications*. Space Technology Library. Kluwer Academic Publishers, El Segundo, California, USA.

Vavasis, S. (1995). Complexity issues in global optimization: A survey. In *Handbook of global optimization*, volume 2, chapter 2, 27–41. Kluwer Academic Publishers.

Yamanaka, K. and Ankersen, F. (2002). New state transition matrix for relative motion on an arbitrary elliptical orbit. *JGCD*, 25(1), 60–66.